Decadal Climate Variability over the North Pacific and North America: Dynamics and Predictability

M. LATIF

Max-Planck-Institut für Meteorologie, Hamburg, Germany

T. P. BARNETT

Climate Research Division, Scripps Institution of Oceanography, La Jolla, California

(Manuscript received 1 May 1995, in final form 5 February 1996)

ABSTRACT

The dynamics and predictability of decadal climate variability over the North Pacific and North America are investigated by analyzing various observational datasets and the output of a state of the art coupled ocean–atmosphere general circulation model that was integrated for 125 years. Both the observations and model results support the picture that the decadal variability in the region of interest is based on a cycle involving unstable ocean–atmosphere interactions over the North Pacific. The period of this cycle is of the order of a few decades.

The cycle involves the two major circulation regimes in the North Pacific climate system, the subtropical ocean gyre, and the Aleutian low. When, for instance, the subtropical ocean gyre is anomalously strong, more warm tropical waters are transported poleward by the Kuroshio and its extension, leading to a positive SST anomaly in the North Pacific. The atmospheric response to this SST anomaly involves a weakened Aleutian low, and the associated fluxes at the air–sea interface reinforce the initial SST anomaly, so that ocean and atmosphere act as a positive feedback system. The anomalous heat flux, reduced ocean mixing in response to a weakened storm track, and anomalous Ekman heat transport contribute to this positive feedback.

The atmospheric response, however, consists also of a wind stress curl anomaly that spins down the subtropical ocean gyre, thereby reducing the poleward heat transport and the initial SST anomaly. The ocean adjusts with some time lag to the change in the wind stress curl, and it is this transient ocean response that allows continuous oscillations. The transient response can be expressed in terms of baroclinic planetary waves, and the decadal timescale of the oscillation is therefore determined to first order by wave timescales. Advection by the mean currents, however, is not negligible.

The existence of such a cycle provides the basis of long-range climate forecasting over North America at decadal timescales. At a minimum, knowledge of the present phase of the decadal mode should allow a "now-cast" of expected climate "bias" over North America, which is equivalent to a climate forecast several years ahead.

1. Introduction

A new and exciting area of climate research is that associated with timescales of a few decades. While many papers have been written on interannual and millennia timescale variations in the planetary climate system, only a few papers have addressed the problem of decadal climate variations. The situation is in contrast to the tremendous importance that climate variability on this timescale has to mankind. Civilization can cope with extreme climate variations that last briefly, say a particularly severe winter. Climate variations with timescales of a millennium are beyond a single human's or even a single political system's lifetime and so elicit little but intellectual interest. But the impact of variations in a key climate variable, say precipitation, that last a decade can generally not be avoided by society, for example, the extended droughts in California, Australia, or the Sahel. The thrust of this paper is to explore and explain physically one particular mode of decadal climate variability that appears in the North Pacific Ocean and its consequences for climate variability over North America. A second goal is to investigate the extent to which this climate mode and its subsequent impacts on North American climate can be predicted.

Two types of decadal Pacific climate variability have been partially described in the literature so far. They may, however, be the same creature. For present purposes we treat them as separate entities, just as they have been treated in the literature. The first is associated with an apparent "shift" in climate mean state or regime that occurred in the mid-1970s. This shift has been extensively described (e.g., Venrick et al. 1987;

Corresponding author address: Dr. M. Latif, Max-Planck-Institut für Meteorologie, Bundesstrasse 55, D-20146 Hamburg, Germany.

Nitta and Yamada 1989; Graham 1994) and aspects of it successfully modeled (e.g., Miller et al. 1994; Graham 1994). Based on an ocean model simulation, Miller et al. (1994) gave a consistent explanation for the physical processes that caused the shift in the North Pacific Ocean, with anomalous horizontal advection, surface heat flux, and mixing being the most important terms in the surface heat budget. Nitta and Yamada (1989) traced the origin of the shift to an abrupt increase in sea surface temperature (SST) of 0.5°–1.0°C in the central and western equatorial Pacific, which is consistent with the conclusion drawn by Graham (1994). At present, no explanation has been put forward as to how this SST increase came about. But in essence, the result in the tropical–extratropical ocean–atmosphere system has been similar to what might be expected during a prolonged, mild warm ENSO extreme, but one that has lasted over a decade.

The second type of decadal change mode appears to be more oscillatory in nature, with a timescale of a few decades. In Fig. 1a, we present low-pass filtered area-averaged North Pacific SST and sea level pressure (SLP) anomalies for the period 1930–1992. Both quantities vary in phase on decadal time scales. The simultaneous fluctuations in the ocean and atmosphere suggest that ocean–atmosphere coupling is important in the generation of the decadal variability.

A 20-yr timescale in Central Californian coastal precipitation was described by Haston and Michaelson (1994), who reconstructed rainfall in this region for the last 600 years. The mode's appearance has been described also in a number of other physical and biological variables [see Trenberth and Hurrell (1994) for a good summary]. It appears to have some features in common with the decadal modes found in the Atlantic sector (e.g., Delworth et al. 1993; Kushnir 1994; Mehta and Delworth 1995) and may be partially responsible for some of the Atlantic decadal variability observed. Perhaps the most comprehensive description of the Pacific mode in the atmosphere has been offered by Trenberth and Hurrell (1994). A description of the mode in the Pacific Ocean has been given by White and Cayan (1996, manuscript submitted to *J. Phys. Oceanogr.*) and Miller et al. (1994). Trenberth and Hurrell (1994) attempt to explain the mode in the atmosphere in terms of the interactions of eddy fluxes of vorticity with the atmospheric mean flow (i.e., the mid-Pacific storm track). The latter quantity is related somehow to changes in the underlaying ocean conditions, but the physics of this connection are not explicitly described, nor has an explanation yet been offered for the presence of this mode in the ocean. Trenberth and Hurrell (1994) conclude by suggesting the fundamental forcing for the decadal mode is to be found in the equatorial Pacific, although midlatitude ocean–atmosphere interactions are important also (although not enumerated). The former part of this explanation is similar to that offered by Graham (1994), whose explanation is more

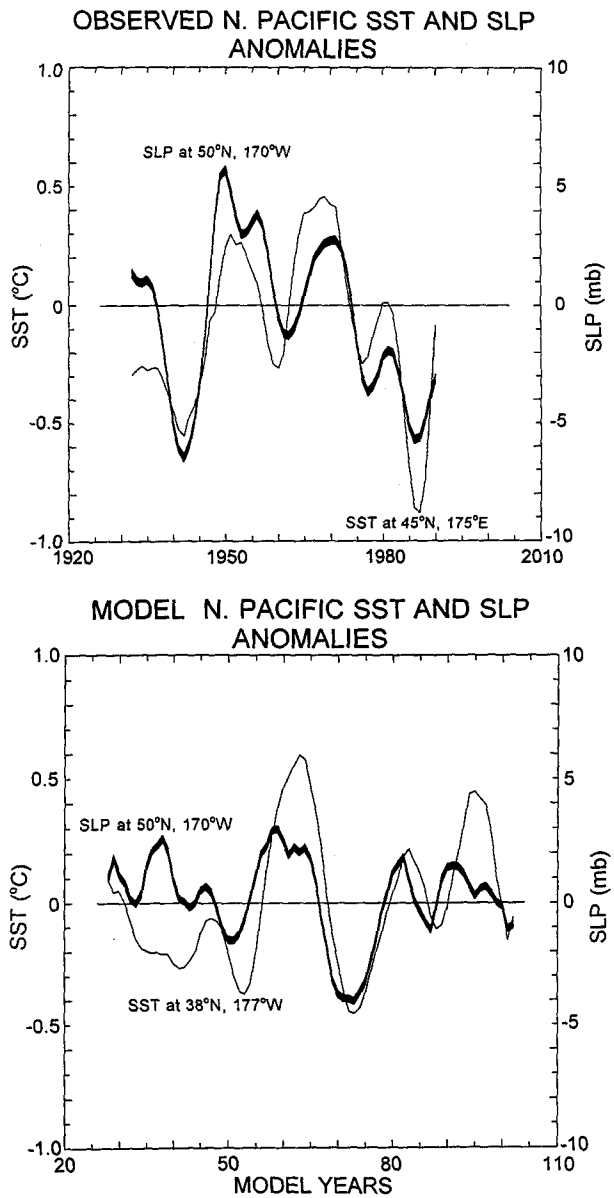

FIG. 1. Low-pass filtered anomalies (retaining variability on timescales longer than 5 years) of North Pacific SST (°C) and SLP (hPa) as (a) observed and (b) simulated by the ECHO CGCM.

firmly based on both numerical model diagnostics and observations. As noted above, there seems to be considerable confusion in the literature as to whether we are dealing with a discrete shift in climate regime or something more oscillatory in nature, the two possibilities often appear to be confounded in any single analysis. It is worth pointing out that this situation is similar to that which existed in the early days of El Niño research.

There seems to be, however, some consensus that midlatitudinal ocean–atmosphere interactions contribute somehow to the decadal variability over the North

Pacific. The possibility of unstable ocean–atmosphere interactions in midlatitudes on seasonal and longer timescales was originally hypothesized by Namias in a series a papers (e.g., Namias 1959, 1969) and by Bjerknes (1964). Namias argued that SST anomalies in the North Pacific can change the transient activity in the atmosphere, which in turn changes the mean westerly flow reinforcing the initial SST anomalies. The paper by Bjerknes is interesting since it postulates a climate cycle with a period of about 10 years in the Atlantic that involves interactions of the westwind regime and the subtropical ocean gyre. As we shall see below, both Namias' and Bjerknes' "early" ideas apply remarkably well to the decadal climate variability over the North Pacific Ocean.

A decadal mode of climate variability in the ocean–atmosphere system of the Pacific has been found in a 125-yr integration of a coupled ocean–atmosphere general circulation model (the ECHAM3 atmosphere model coupled to the HOPE ocean model, hereafter referred to as ECHO, described in section 2). A preliminary description of this mode and the physics responsible for it has been given by Latif and Barnett (1994). Suffice to say, it has many of the features of the observed decadal mode(s) discussed above (see, for instance, Fig. 1b). The goals of this study are to describe the decadal variability more fully, but not only in terms of the model results but also by observations (section 3). More important will be to offer a physical explanation for its existence in both the ocean (section 4) and the atmosphere (section 5). The impact of this mode on the climate over North America and the predictability of this impact are discussed in section 6. The conclusions resulting from our study are given in section 7.

2. Coupled model and observational data

a. Coupled model

The coupled model and its behavior with respect to climate drift and interannual variability during the first 20 years of the integration are described in Latif et al. (1994a). The atmospheric component of our coupled GCM "ECHO" is ECHAM-3, the Hamburg version of the European Centre for Medium-Range Weather Forecasts operational weather-forecasting model. The model is described in detail in two reports (Roeckner et al. 1992; DKRZ 1992). ECHAM-3 is a global low-order spectral model with a triangular truncation at wavenumber 42 (T42). The nonlinear terms and the parameterized physical processes are calculated on a 128×64 Gaussian grid, which yields a horizontal resolution of about $2.8° \times 2.8°$. There are 19 levels in the vertical, which are defined on σ-surfaces in the lower troposphere and on p-surfaces in the upper troposphere and in the stratosphere.

The ocean model is "HOPE" (Hamburg Ocean Model in Primitive Equations), which is based on primitive equations (see Latif et al. 1994a and references therein). Its domain is global and we use realistic bottom topography. The meridional resolution is variable, with 0.5° within the region 10°N to 10°S. The resolution decreases poleward to match the T42-resolution of the atmosphere model. The zonal resolution is constant and also matches the atmospheric model resolution. Vertically, there are 20 irregularly spaced levels, with 10 levels within the upper 300 m. Since we have not yet included a sea ice model in HOPE, the SSTs and sea surface salinities are relaxed to the climatology of Levitus (1982) poleward of 60°, using Newtonian formulations with time constants of about 2 and 40 days, respectively, for the upper-layer thickness of 20 m. The vertical mixing is based on a Richardson-number-dependent formulation and a simple mixed-layer scheme to represent the effects of wind stirring (see Latif et al. 1994a for details).

The two models were coupled without flux correction. They interact over all three oceans in the region 60°N–60°S. The ocean model is forced by the surface wind stress, the heat flux, and the freshwater flux simulated by the atmosphere model, which in turn is forced by the SST simulated by the ocean model. The coupling is synchronous, with an exchange of information every two hours. The coupled GCM is forced by seasonally varying insolation. The coupled integration is started at 1 January and continued for 125 years.

In order to reduce spinup problems, we omit the first 20 years of the integration (which are described in Latif et al. 1994a) in the discussion of the decadal variability. Overall, the drift is reasonably small during the last hundred years of the coupled integration with ECHO, especially in the North Pacific. This is demonstrated by the linear trend coefficients that were computed over the last hundred years of the coupled integration (Fig. 2). Some serious model drift, however, is found in the North Atlantic, which cools by about 1°C during the last 100 years. This was expected because the 15-yr spinup integration with the HOPE model is much too short to bring the thermohaline circulation into equilibrium. In the other regions, however, most of the errors develop during the first 20 years of the coupled integration. The spatial structure of this initial model drift is shown in Latif et al. (1994a, their Fig. 1c). In particular, simulated annual mean SSTs in the North Pacific are typically 1°–2° too cold. In summary, the coupled model is rather stable during the analyzed period of years 21–125. This is also confirmed by Fig. 1b showing indices of SST and SLP simulated over the North Pacific.

b. Observational data

A variety of observational data will be used in subsequent sections of this paper. A short description of these data is given below. In all cases, the data were regridded from their original grid to the T42 grid of the

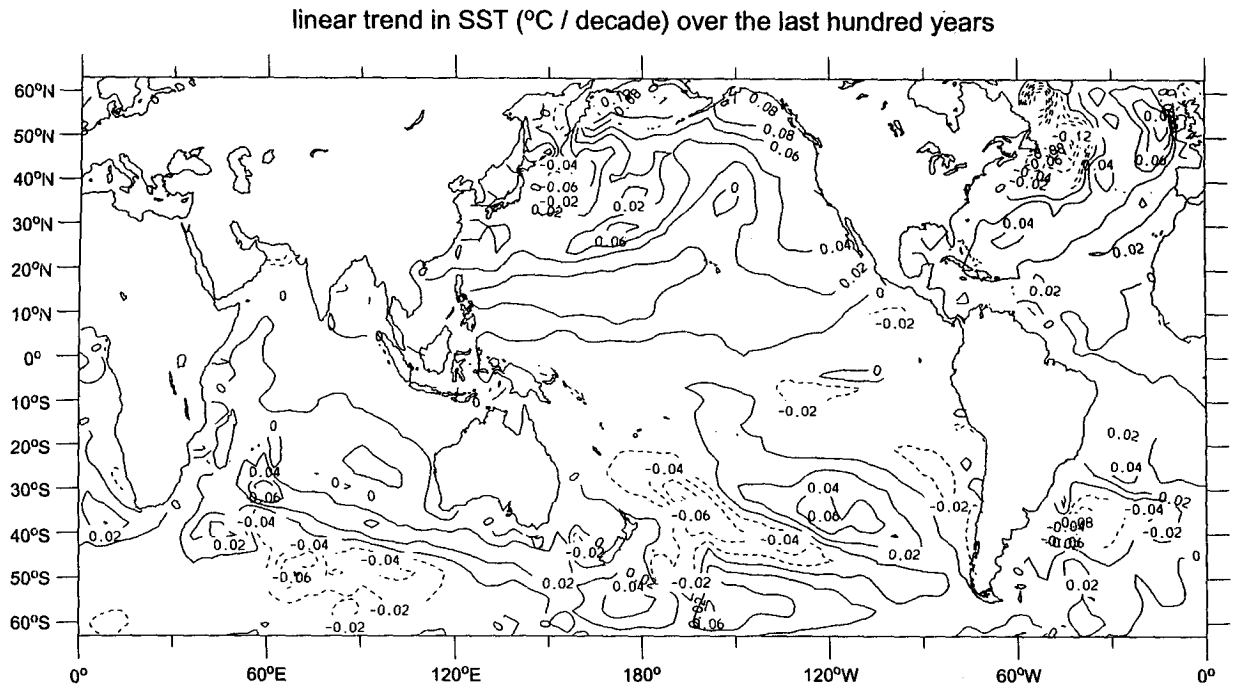

FIG. 2. Spatial distribution of linear trend coefficients of SST (°C decade^{-1}) in the coupled integration during model years 26 and 125. The contour interval is 0.02 °C decade^{-1}.

AGCM component of ECHO. All data were available at monthly intervals.

Sea surface temperature (SST) data were obtained from three sources. Recent SST fields were obtained from the Climate Analysis Center (NOAA) and are described by Reynolds (1988). Prior to 1970 we have used the COADS data (Slutz et al. 1985) and additionally the SST dataset of the British Meteorological Office (UKMO), which is referred to as the "GISST" dataset, covering the period 1949–1991. We note that the three datasets were used individually and not combined into one dataset.

Sea level pressure (SLP) data were taken from the near-global product described by Barnett (1985) for the period after 1955. Prior to that time the Historical Map Series (Jenne 1975) for the Northern Hemisphere provided the required data. Additionally we used Northern Hemisphere 700-hPa heights for the period 1949–1991, which were provided by the Climate Analysis Center.

Near-surface air temperature over North America was obtained from an update of the Climate Research Unit (CRU) product (Jones et al. 1986). This record will be used back to 1866. Inspection of the individual monthly maps for the era showed a surprising amount of information in the regions wherein the decadal mode we will be discussing has maximum variance. Therefore we have some confidence in the results for the whole period 1866–1992.

Rainfall, in gridded field format, was also provided courtesy of the CRU (cf. Hulme and Jones 1993). Comparison of these data with the United States divisional data and individual data suggest they are valid in the main areas of interest back to 1900.

Heat content of the upper 400 m of the North Pacific Ocean was provided courtesy of W. White (cf. White and Cayan 1996, manuscript submitted to *J. Phys. Oceanogr.*). This set was obtained by combining all mechanical and expendable bathythermograph (BT) data with all the hydrographic data taken in the North Pacific in an objective analysis. The result were fields of ocean temperature gridded horizontally at 2° × 2° resolution and at selected depths levels down to 400 m. In the current analysis, only monthly data back to 1970 were used since the mechanical BT data from earlier times are subject to systematic errors.

3. Description of model variability and comparison with observations

In order to investigate the coupled model's ability to simulate the decadal variability over the North Pacific, we compare the two leading empirical orthogonal functions (EOFs) of low-pass filtered SST anomalies derived from the observations for the period 1970–1992 (Fig. 4) with those derived from the coupled integration with ECHO (Fig. 3). The first two leading EOFs derived from the data explain together about 57% of

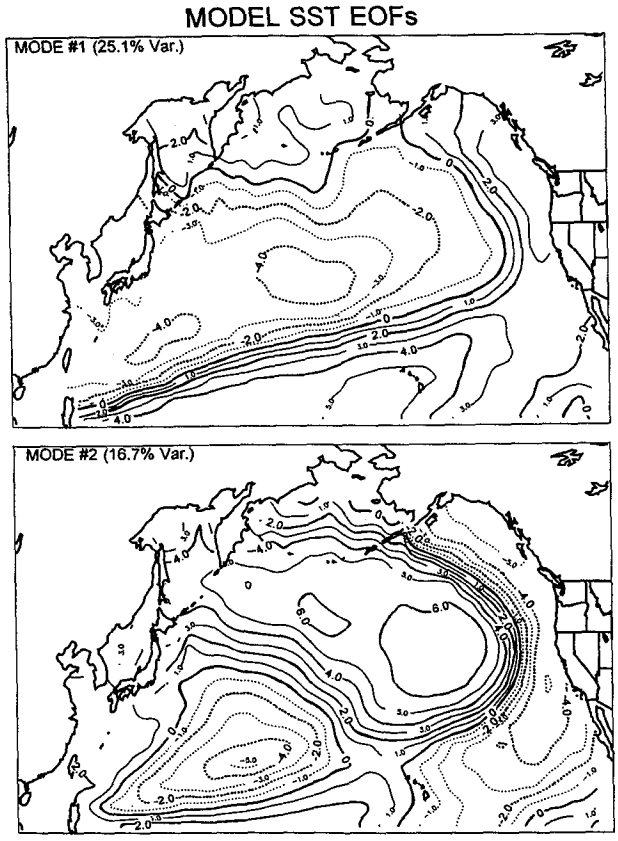

FIG. 3. First two EOFs of coupled model SST anomalies in the North Pacific. The anomalies were smoothed with a 3-yr running mean filter and detrended prior to the EOF analysis. The units are arbitrary. Since the variances of the corresponding principal components are similar to those derived from the observations, the EOF patterns can be compared directly to those presented in Fig. 4.

the variance, while those from the coupled model account for about 42% of the model variance. The coupled model shows reasonable skill in reproducing the main variability patterns observed, but the relative ranking of the two leading EOFs is reversed in the model. However, it should be kept in mind that the results of the EOF analysis for the observed SST anomalies are subject to large uncertainties due to the relatively short record used. The relative ranking of the two leading EOFs for the observed SST anomalies reverses when the EOFs are computed from the GISST dataset covering the period 1949–1991.

The leading EOF of the model SST anomalies (Fig. 3, upper) is characterized by an anomaly that covers almost all of the North Pacific. As we shall see below, this mode represents the decadal mode in question. The main SST anomaly is tilted from the southwest to the northeast and has maximum values along the path of the model Kurushio Current. The main SST anomaly is surrounded by anomalies of opposite sign, most prominently to its south. Basically the same features are found in the second EOF of the observed SST anomalies (Fig. 4, upper). The second model EOF (Fig. 3, lower) shows a dipole structure, with centers of action in the southwestern and northeastern part of the North Pacific. This EOF mode shares some similarities with the first EOF mode of the observations (Fig. 4, lower), but the positive anomaly is located farther to the north in the model simulation.

We performed a Canonical Correlation Analysis (CCA) between low-pass filtered (retaining variability on timescales longer than 5 years) SST and 500-hPa height anomalies in order to derive the leading modes of ocean–atmosphere covariability. We did not restrict the CCA to the North Pacific only because we are also interested in the teleconnections associated with the North Pacific mode. The leading CCA mode is associated with the slow climate drift of the coupled model. The SST pattern of this mode is similar to the pattern shown in Fig. 2 and will not be discussed further. The second CCA mode represents the decadal mode in question. Its canonical correlation (r^2) amounts to 0.91, and the two canonical time series are very similar to the time series shown in Fig. 1b and are therefore not shown. The variance explained by the second CCA

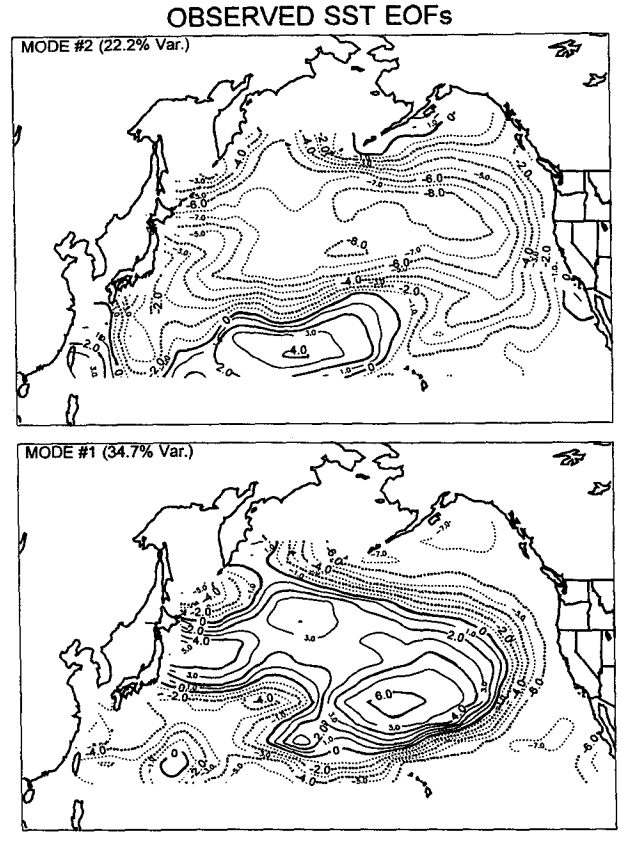

FIG. 4. First two EOFs of observed SST anomalies in the North Pacific. The anomalies were smoothed with a 3-yr running mean filter and detrended prior to the EOF analysis. The units are arbitrary.

mode amounts to about 24% relative to the SST data and 29% relative to the 500-hPa data. The third CCA mode that will be discussed in a forthcoming paper is associated with the decadal variability in the central North Atlantic.

The canonical SST pattern of CCA mode 2 (Fig. 5a) exhibits strongest anomalies in the North Pacific. The structure of the anomalies in this region is very similar to that of EOF 1 (Fig. 3a), with maximum anomalies at about 40°N in the vicinity of the date line. Please note also the strong meridional gradient in the SST anomaly field between 25° and 35°N, which is more likely to affect the atmospheric circulation than the SST anomalies themselves (White and Barnett 1972). The local explained variances in the North Pacific are typically of the order of 30%–50% relative to the low-pass filtered SST data and up to about 80% in the center of the warm anomaly.

Three features outside the North Pacific deserve special attention. First, we find a pronounced symmetry about the equator in the Pacific. Although the positive SST anomalies in the Southern Pacific are less strong than those in the North Pacific, the explained variances amount to about 50% in the centers of action. Second, a rather strong positive anomaly is found in the subtropical Atlantic centered near 35°N. This anomaly accounts for a considerable fraction of the total low-frequency variance in the subtropical Atlantic. The Atlantic decadal variability will be described in a forthcoming paper. Third, SST anomalies in the equatorial Pacific are of opposite sign relative to the main anomaly in the North Pacific and relatively weak, which suggests that the decadal mode has its origin in midlatitudes.

The anomalous atmospheric circulation associated with CCA mode 2, as expressed by the 500-hPa anomaly field (Fig. 5b), is dominated by the reverse of the "Pacific–North American" (PNA) pattern, which is an eigenmode of the atmosphere and also excited during extremes of the El Niño–Southern Oscillation (ENSO) phenomenon (Horel and Wallace 1981). The anomalies associated with the PNA pattern are highly significant, with explained variances relative to the low-pass filtered height anomalies of about 90% in the center of the Aleutian anomaly and about 60% in the centers farther downstream. As for the SST, we find also in the height field some symmetry about the equator and a significant response over the subtropical Atlantic.

The results of the CCA between model SST and the 500-hPa height anomalies derived from the coupled model simulation show clearly that ocean and atmosphere over the North Pacific vary coherently in phase, which suggests that ocean–atmosphere interactions are important. Our coupled model results are consistent with observations over the North Pacific, which show also that ocean and atmosphere vary coherently in phase on decadal timescales (Fig. 1a). Additionally we

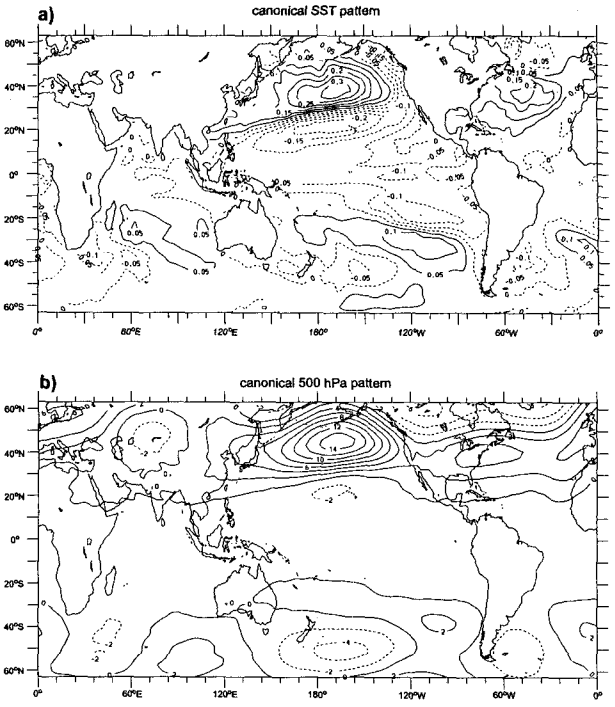

FIG. 5. Results of a Canonical Correlation Analysis (CCA) between coupled model SST and 500- hPa height anomalies. Shown are (a) the canonical predictor (SST) and (b) canonical predictand (500 hPa) patterns of CCA mode 2. The values are representative of a one standard deviation change. The units are degrees Celsius and geopotential meters, respectively. The data were smoothed with a 5-yr running mean filter prior to the analysis, and five EOFs were used in each field.

performed a correlation analysis of low-pass filtered SST and 700-hPa height anomalies observed during the period 1949–1991. The correlation analysis was performed as follows. First, the observations were detrended and smoothed with a 5-yr running mean filter. We then defined a SST index by averaging the SST anomalies over the region 25°–40°N and 170°E–160°W (Fig. 6a). This particular region was chosen because it is located in the region of maximum decadal variability. Then we computed locally the correlation coefficients of the SST index with the SST and 700-hPa anomalies that were preprocessed in the same way as the SST index.

The results of the correlation analysis are shown in Figs. 6b and 6c. They are consistent with the coupled model results: the dominant SST anomaly in the North Pacific is positive (by definition) and surrounded by negative anomalies (Fig. 6b), and anomalously high pressure is found over anomalously warm SSTs (Fig. 6c), a result that was found also by Trenberth and Hurrell (1994). These features are highly significant, as are those in the coupled model data. As in the coupled model simulation, there is a small-scale equatorial Pacific SST anomaly of opposite sign to the main North Pacific anomaly, and the SST anomaly pattern shows

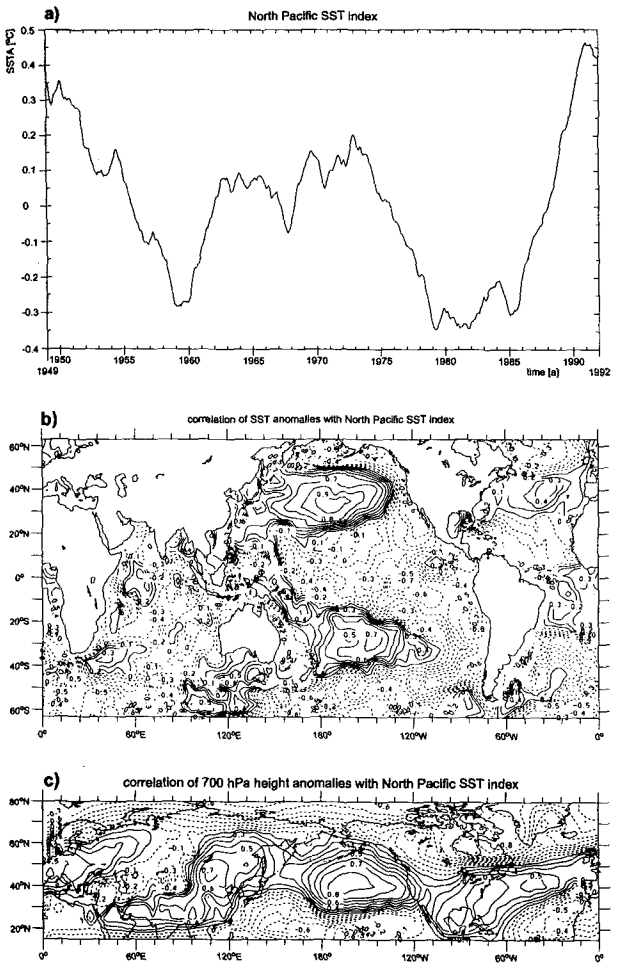

FIG. 6. (a) Time series of North Pacific SST anomalies averaged over the region 25°–40°N, 170°E–160°W and spatial distributions of correlation coefficients of (b) observed SST anomalies and (c) observed 700-hPa height anomalies with the index time series shown in (a). All data were detrended and smoothed with a 5-yr running mean filter prior to the correlation analysis.

some symmetry about the equator. The PNA signature over the North Pacific and North America is also found in the observations, and the correspondence over the North Atlantic between the coupled model and the observations is reasonably good. Thus, the observations support also the picture that the origin of the decadal mode is in midlatitudes and equatorial Pacific SST anomalies play a minor role in the dynamics of the decadal mode.

4. Physics of the atmospheric response

Our hypothesis for the cause of the decadal variability over the North Pacific is that it arises from an instability of the coupled ocean–atmosphere system over the North Pacific. Thus, we believe that the decadal variability is an inherently coupled phenomenon. Furthermore, we believe that the Tropics are of minor importance for the generation of the decadal variability, which is completely different from the hypotheses offered in most other studies (e.g., Trenberth and Hurrell 1994; Graham 1994; Jacobs et al. 1994). In order to prove these claims, we conducted a series of analyses that are described in the following sections.

The results shown above raise the question as to whether there exists a significant response of the atmospheric circulation to midlatitudinal SST anomalies. This is an issue that is very controversial. On the one hand, many studies concluded that the atmosphere is essentially insensitive to midlatitudinal SST anomalies (e.g., Graham 1994; Lau and Nath 1994). On the other hand, some other studies support the picture that midlatitudinal SST anomalies do force significant changes in the atmospheric circulation (e.g., Palmer and Sun 1985; Brankovic et al. 1994). In order to further address this question, we performed sensitivity experiments with our atmospheric general circulation model (AGCM) ECHAM-3 forced by prescribed SST anomalies in stand-alone integrations. Before we continue the discussion of the results of the coupled model, we briefly describe the results from the uncoupled experiments with our atmosphere model.

a. AGCM sensitivity experiments

In a first experiment, we forced our AGCM by a SST anomaly pattern that is very similar to the first EOF of low-pass-filtered SST anomalies derived from the coupled model integration (Fig. 3, upper). The pattern of the anomalous SST forcing was derived from a regression analysis and is shown in Latif and Barnett (1994) (see also Fig. 8, upper). We scaled the SST pattern in such a way that maximum SST anomalies are of the order of 1°C. We performed an 18-month perpetual January integration, and the first three months were omitted in the analysis of the experiment in order to eliminate spinup problems. In a second experiment, we repeated the first experiment, but with the signs of the SST anomalies reversed. For comparison, we performed a control experiment with climatological January SSTs. The control experiment was performed in the same way as the sensitivity experiments and starts also from the same initial conditions that were taken from a multiyear control integration with ECHAM-3 forced by seasonally varying SST.

As shown in Latif and Barnett (1994), we found indeed a significant response of the atmospheric circulation to the prescribed SST anomalies, and we were able to reproduce the anomalous 500-hPa height pattern derived from the coupled integration (Fig. 5b). This was also true when we repeated the experiments with all SST anomalies south of 25°N set to zero, which indicated that tropical SST anomalies played a minor role in the result and demonstrated that midlatitudinal SST anomalies can force significant changes in the

large-scale atmospheric circulation. Here we show the response in terms of sea level pressure and 2 m air temperature (T-2 m) and compare them with observed decadal-scale anomalies (Figs. 7 and 8), which were composited with respect to the low-pass-filtered North Pacific SST anomalies (Fig. 1a). In order to enhance the signal, we show the results for both the model (Figs. 7 and 8 upper panels) and data (Fig. 7 and 8 middle and lower panels) as differences between the high and low SST extremes. The AGCM reproduces reasonably well the observed SLP changes, with strongest anomalies in the Aleutian low region (Fig. 7). The T-2 m response over North America farther downstream is also similar in both the model and observational results, with cold anomalies in the northwest and warm anomalies in the southeast.

We note that the model response shown here is considerably weaker relative to that presented in Latif and Barnett (1994), which was based on 12 January, and the positive SST extreme only and almost twice as large. The high internal variability of the midlatitudinal atmosphere demands large ensembles in order to reduce sampling problems (e.g., Barnett 1995). The additional integrations using warm and cold SST anomalies lead now to a mean response that is much weaker relative to that presented in Latif and Barnett (1994) and in good agreement with the observations. Our results strongly support the picture that the atmosphere is sensitive to midlatitudinal SST anomalies. This is also supported by an experiment performed at the National Meteorological Center (Kumar 1995, personal communication) in which the same SST anomaly pattern served as forcing as that we used. Kumar was able to reproduce our results, although with somewhat weaker amplitude. A detailed analysis of the AGCM sensitivity experiments, however, is beyond the scope of this paper since we are interested here in the dynamics of the coupled ocean–atmosphere system over the North Pacific.

b. *Surface fluxes*

We now continue the discussion of the results simulated by the coupled model. Of particular importance are the anomalous surface fluxes that drive the ocean. In order to derive the characteristic heat flux and surface wind stress anomalies that are associated with the decadal mode, we computed locally the corresponding linear regression coefficients relative to the canonical time series of the canonical SST pattern shown in Fig. 5a. Prior to the regression analyses, the surface heat flux and zonal wind stress anomalies were smoothed with a 5-yr running mean filter.

The surface heat flux pattern shows over the North Pacific mainly positive anomalies to the west and mostly negative anomalies to the east of the date line (Fig. 9a). Thus, SST anomalies are reinforced in the western, while they are damped in the eastern Pacific

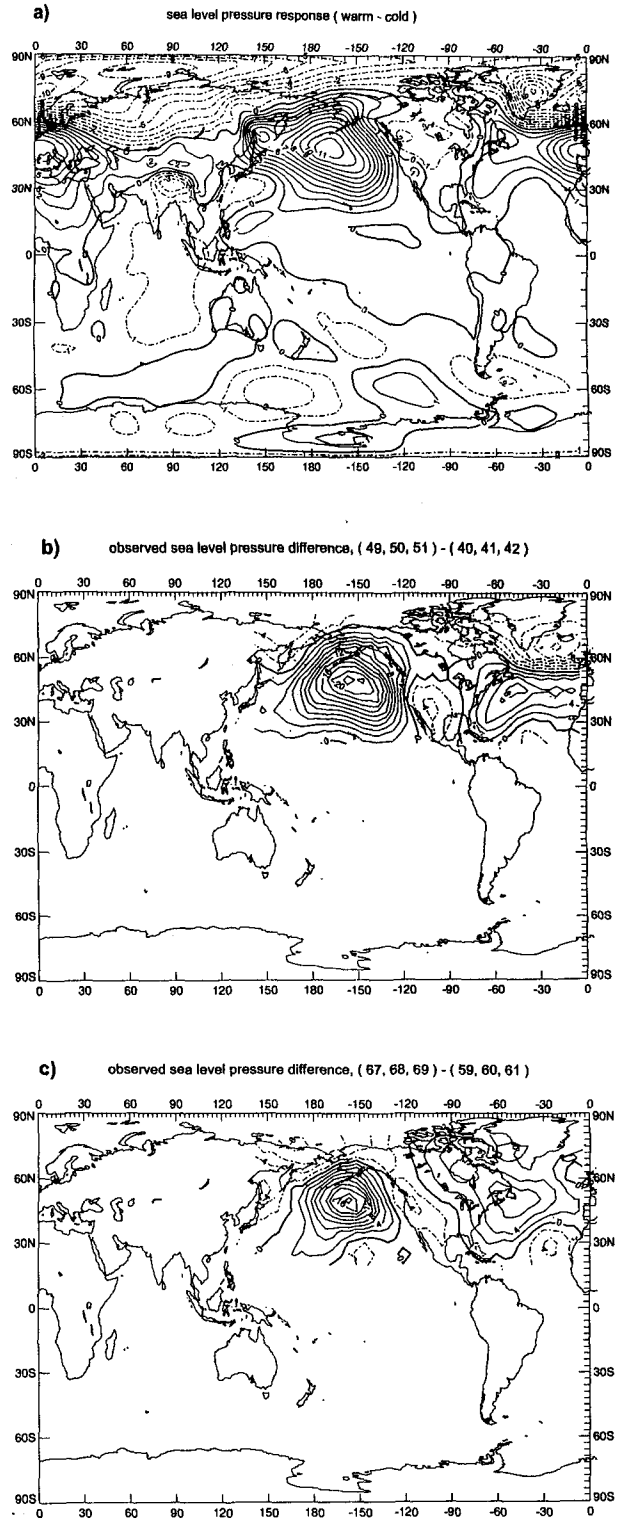

FIG. 7. Difference of January SLP anomalies (hPa) between high and low SST extremes in the North Pacific. (a) Response of the ECHAM-3 AGCM to the SST anomaly pattern shown in Fig. 8a; (b) difference of observed January SLP anomalies averaged over the years 1949–1951 and 1940–1942; (c) difference of observed January SLP anomalies averaged over the years 1967–1969 and 1959–1961.

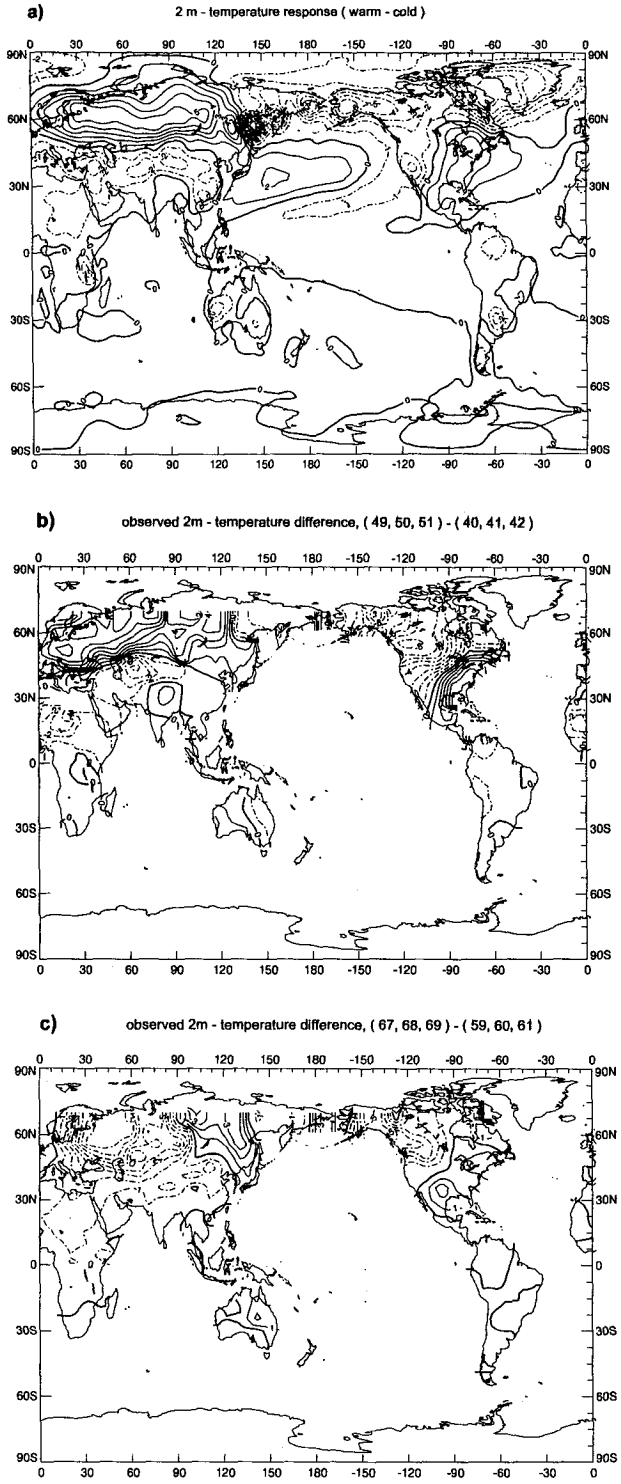

FIG. 8. Difference of January near-surface temperature anomalies (°C) between high and low SST extremes in the North Pacific. (a) Response of the ECHAM-3 AGCM to the SST anomaly pattern imposed over the North Pacific, (b) difference of observed January near surface temperature anomalies averaged over the years 1949–1951 and 1940–1942, (c) difference of observed January near surface temperature anomalies averaged over the years 1967–1969 and 1959–1961.

by the net surface heat flux. Typical decadal-scale heat flux anomalies are of the order of a few watts per squared meter, and the local explained variances are of the order of about 30% in the centers of action over the North Pacific. The main components in the surface heat balance are the sensible and latent heat fluxes, while radiative fluxes are rather small (not shown). The heat flux pattern is largely consistent with the pressure patterns presented in Figs. 5, 6, and 7 showing an anomalous high pressure system over the North Pacific that will result in anomalous warm-air advection over the western and anomalous cold-air advection over the eastern Pacific.

In Fig. 9b, we present the associated zonal wind stress pattern. Local explained variances relative to the low-pass filtered values are of the order of 60% in the anomaly centers over the North Pacific. The zonal wind stress pattern over the North Pacific is dominated by a dipole structure, with strongest negative anomalies in the vicinity of the main SST anomaly and positive anomalies farther north. Thus, the westerlies are shifted northward and they are considerably weakened in the region of the positive SST anomaly. The changes in the zonal wind stress will lead to reduced wind mixing in the ocean and to anomalously strong Ekman heat transport, and both changes will act as a positive feedback on the SST anomalies across the North Pacific, which is consistent with the model study of Miller et al. (1994).

The changes in the wind stress curl over the central Pacific are mainly given by the meridional shear of the zonal wind stress anomaly. Most important for the subtropical gyre circulation is the positive curl anomaly in the subtropics between about 20° and 35°N, which weakens the mean negative wind stress curl in this region and will tend to spin down the gyre and reduce the poleward heat transport by the Kuroshio and its extension. As described below, the ocean adjustment to variable wind stress involves the propagation of planetary waves, and the variations in upper-ocean heat content as simulated by our coupled model are consistent with this picture.

5. Physics of the oceanic response

We now discuss the ocean physics involved in the decadal mode using the coupled model data. In particular, we are interested in the question of how the phase reversal between warm and cold phases of the decadal mode comes about. We shall show that the memory of the coupled system resides in the ocean and that the transient response of the North Pacific to the above described changes in the wind stress curl is essential for the generation of the decadal mode. First, we performed a combined POP (Principal Oscillation Pattern) analysis (Hasselmann 1988; von Storch et al. 1995) using SST and ocean heat content anomalies of the upper 400 m. Prior to the POP analysis, the data were

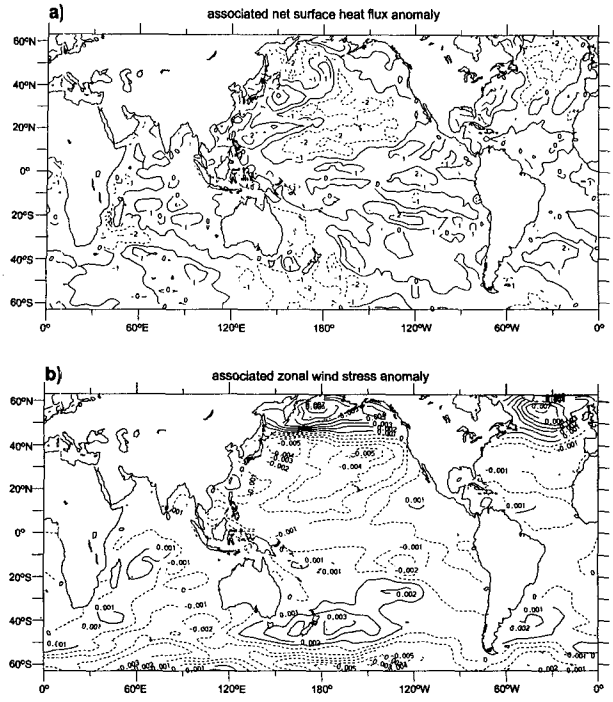

FIG. 9. Spatial distribution of linear regression coefficients of net surface heat flux and zonal wind stress anomalies relative to the time series of the canonical SST pattern shown in Fig. 5a. (a) Net surface heat flux pattern (W m^{-2}). Positive values indicate fluxes into the ocean and (b) zonal wind stress wind pattern (N m^{-2}). The values are representative of a one standard deviation change in the decadal mode. The data were smoothed with a 5-yr running mean filter prior to the analyses.

low-pass filtered (retaining variability on timescales longer than 5 years), detrended, and divided by their local standard deviation. The leading POP mode, explaining about one-quarter of the low-frequency variance in the combined dataset, is the decadal mode under consideration. Its POP period amounts to about 30 years and its damping time to about 15 years. We note, however, that timescale estimates from such a short record are subject to large uncertainties and sensitive to the method of computing the POP period (e.g., Barnett et al. 1995).

The evolution of the anomalies according to a single (complex) POP mode with real part Re and imaginary part Im can be interpreted as a cyclic sequence of patterns:

$$\ldots \rightarrow \mathrm{Im} \rightarrow \mathrm{Re} \rightarrow -\mathrm{Im} \rightarrow -\mathrm{Re} \rightarrow \mathrm{Im} \rightarrow \ldots .$$

The evolution of SST anomalies derived from this POP mode can be basically described as a standing oscillation, with a rather strong real part (Fig. 10b) and a relatively weak imaginary part (Fig. 10a). Some evolutionary behavior, however, can be seen. SST anomalies in the western subtropical Pacific (Fig. 10a) precede those in the central North Pacific (Fig. 10b) by one-quarter of the POP period, that is, several years. The propagation of anomalies along the Kuroshio Extension can be seen more clearly in the corresponding heat content patterns (Fig. 11). Heat content anomalies cover a considerable part of the western and central subtropical Pacific (Fig. 11a) prior to the development of the SST and heat content anomalies in the central North Pacific (Figs. 10b and 11b). The heat content anomalies tend to propagate in a clockwise manner around the Pacific, reminiscent of the gyral circulation. Further analysis revealed that the vertical structure of the anomalies is consistent with that of the first baroclinic mode.

Consider, for instance, the real part that is the negative extreme phase of the decadal mode (Fig. 11b). Positive heat content anomalies can be seen south of the negative anomalies at this time. These negative anomalies that have reached the western boundary in the southernmost part of the region considered "reflect" and propagate northward and eastward, as indicated by the rotation from the real to the (negative) imaginary part (Fig. 11a, but with reversed signs). The positive anomalies expand in a northeastern direction, as revealed by the rotation from the (negative) imaginary part to the (negative) real part (Fig. 11b, but with reversed signs), which completes the phase reversal.

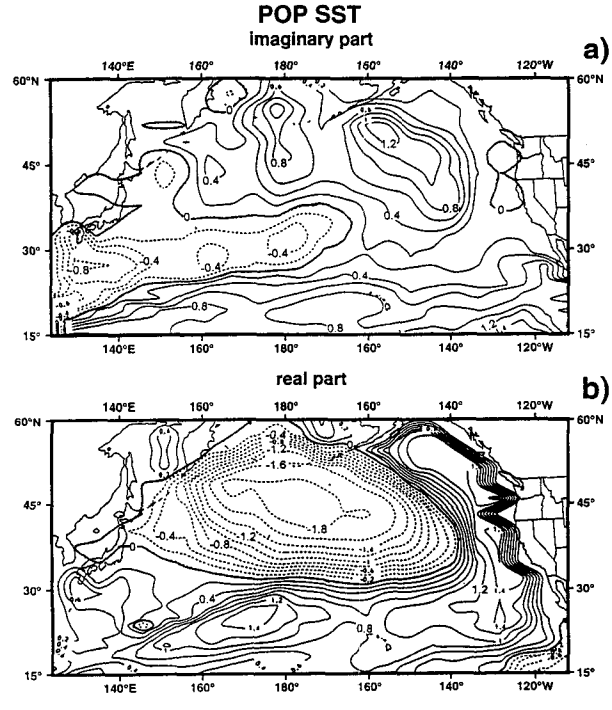

FIG. 10. Results of a combined POP analysis of coupled model SST and heat content anomalies. (a) Imaginary part of SST, (b) real part of SST. The data were low-pass filtered with a 5-yr running mean and normalized by their local standard deviation prior to the POP analysis.

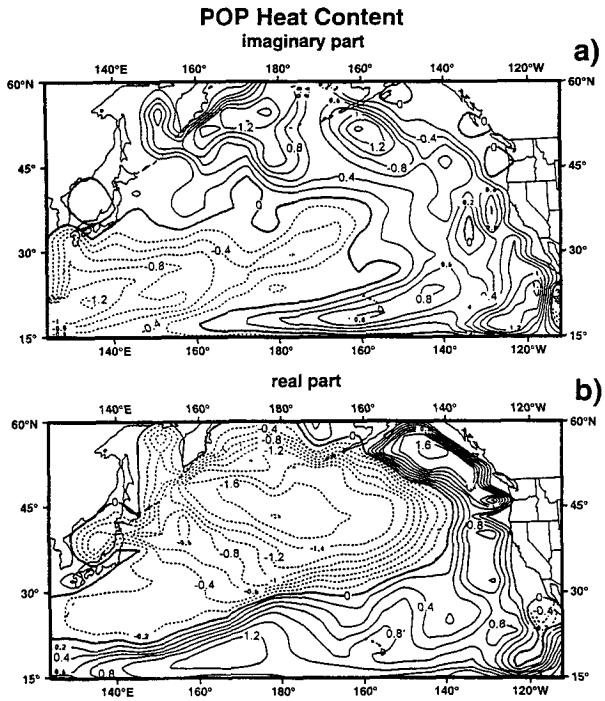

FIG. 11. Results of a combined POP analysis of coupled model SST and heat content anomalies. (a) Imaginary part of heat content, (b) real part of heat content. The data were low-pass filtered with a 5-yr running mean and normalized by their local standard deviation prior to the POP analysis.

Thereafter, the whole sequence of events starts over again, but with reversed signs.

The evolution in the upper ocean heat content as derived from the leading POP mode can be explained in principal by both planetary wave propagation and heat advection by mean currents. The transient response of a midlatitudinal ocean to variable wind stress was investigated in many theoretical and modeling studies (e.g., Anderson and Gill 1975; Anderson et al. 1979; Gill 1982). The response is mainly baroclinic at timescales of more than several months and involves the propagation of long, relatively fast planetary waves with westward group velocity and the propagation of short, relatively slow planetary waves with eastward group velocity. The net effect of the planetary wave propagation is to modify the strength of the subtropical gyre and its associated poleward heat transport, which leads eventually to the generation of SST anomalies in the North Pacific. The spinup time of the gyre is of the order of several years, which can explain the decadal timescale of the mode.

This picture, however, is complicated by the presence of the mean currents. Advection of heat by the mean currents is likely to contribute also to the ocean adjustment. In order to distinguish between the wave and the advection scenarios that represent two extremes in parameter space, we computed the surface heat budget for the location 35°N, 180° in the central Pacific. The results of the heat budget calculation are not very sensitive to the precise location used. We note, however, that the results are based on annual mean values that were stored only. A complete heat budget analysis is given by Xu et al. (1996 manuscript submitted to *J. Climate*), who reran particular periods of the model simulation and outputted the different tendendy terms with higher temporal resolution.

Of particular interest here are the two terms $u'\partial\bar{T}/\partial x$ and $\bar{u}\partial T'/\partial x$. The first tendency includes the effects of planetary wave activity, while the latter one arises from advection by the mean currents. We restrict ourselves here to the zonal components only because they dominate the meridional ones in this part of the North Pacific. The two tendencies are shown together with the anomalous wind stress curl farther south at 20°N, 180° in Fig. 12. The wind stress curl anomaly in this region varies in phase with the SST anomaly in the North Pacific. Although both tendencies are of the same order of magnitude, only the temperature advection by the anomalous currents shows a fairly consistent phase relationship with the wind stress curl anomaly, the latter lagging by about 5 years. This indicates that the wave adjustment is the more important component in the phase reversal, but with the caveat that the heat advection by the mean currents is not negligible. Additional correlation analyses revealed that the atmospheric forcing terms (heat flux and wind stress) do not contribute to the phase reversal.

In summary, our results support the picture that the decadal mode arises from unstable ocean–atmosphere interactions over the North Pacific. The memory of the coupled system resides in the ocean, while the atmosphere responds passively to the slowly varying boundary conditions. It is interesting to note that this paradigm for the generation of the decadal variability over the North Pacific is similar to that for the ENSO phenomenon in the tropical Pacific (e.g., Schopf and Suarez 1988).

6. Implications for decadal predictability

The paradigm we developed for the decadal variability over the North Pacific implies the possibility to predict decadal climate anomalies over North America. Both the coupled model and the observations show a strong, simultaneous wintertime relation between low-pass-filtered anomalies of atmospheric pressure in the heart of the main atmospheric response region, south of the Aleutians, and air temperature over North America (Fig. 13). Negative anomalies of temperature over the northern part and positive anomalies of temperature over the southern part of the continent go with higher than normal pressure in the Aleutians. This relationship basically reflects the anomalies that are expected from the Pacific North American (PNA) pattern, which is a crucial part of the decadal mode. In the heart of the

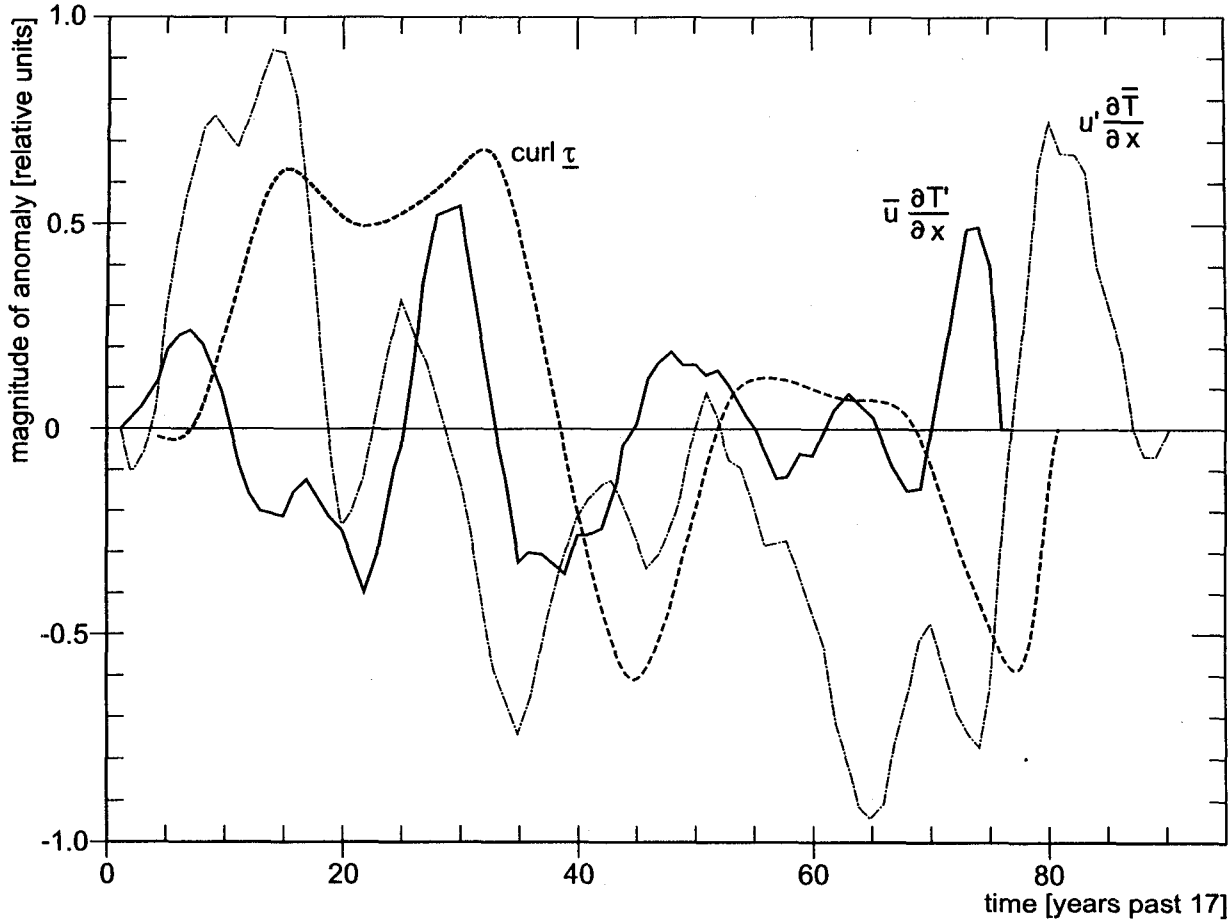

FIG. 12. Anomaly time series of the advection of mean temperature by anomalous current ($u'\partial\bar{T}/\partial x$) and anomalous temperature by mean currents ($\bar{u}\partial T'/\partial x$) at 35°N, 180° and the wind stress curl at 20°N, 180°. The time series were smoothed with a 5-yr running mean filter. The two temperature tendencies were scaled in the same way so that they can be compared directly.

high correlation regions, the decadal mode accounts for 35%–65% of the variance of the low-pass filtered observed temperature data. Significant correlations are also found between observed anomalies of pressure south of the Aleutians and precipitation over North America (Fig. 14b). The coupled model, however, fails to reproduce this relationship (Fig. 14a), which reflects the problems of state of the art AGCMs to realistically simulate rainfall.

We can make use of these strong relationships to derive indices of decadal variability over the North Pacific that extend back into the last century in the case of the surface air temperature and to the turn of the century in the case of precipitation. The strategy we adopted is to take observed gridded winter data over North America and to project them onto the characteristic response patterns shown in Figs. 13 and 14. This yields "pseudo" principal components that can be regarded as indices of the strength of the decadal variability over the North Pacific (Fig. 15). The two time series vary together in phase and show some indication of oscillatory behavior, with a preferred timescale and about 20 years, which was inferred from the corresponding autocorrelation functions (Fig. 18 shows the autocorrelation function of the near surface temperature pseudo principal component).

These facts suggest the possibility of predicting climate variability over the North American continent provided we can predict the behavior of the mode in the Pacific. The fraction of variance associated with the decadal mode in the observed seasonal temperature and precipitation fields is large enough (35%–65%) to suggest these predictions would be practically useful; especially if they are added to the predictive skill associated with ENSO extremes (e.g., Latif et al. 1994b, Barnett et al. 1994). The word "prediction" as used here has two senses: (i) it means predicting the phase of the decadal mode years in advance, which is equivalent to predicting the onset of the prolonged period of, say, above or below rainfall over the western United States, (ii) due to the slow evolution of the mode, one might determine its current phase and simply make a

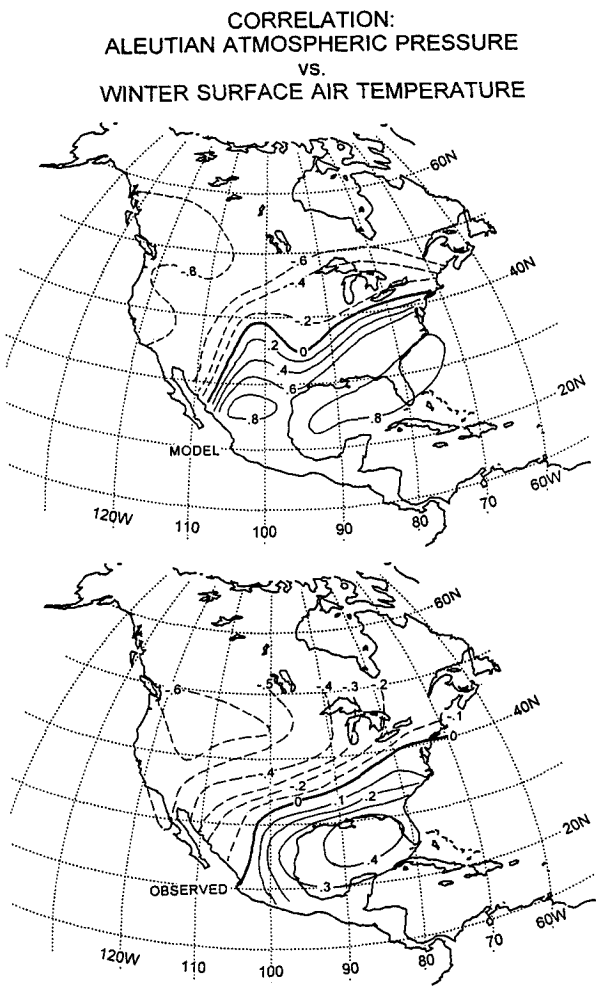

FIG. 13. Correlation of winter sea level pressure anomalies in the Aleutian low region with near surface temperature anomalies over North America. (a) Upper, as simulated by the ECHO CGCM. (b) Lower, as derived from observations. The contour interval in the upper panel is 0.2 and that in the lower diagram 0.1.

"decadal nowcast" of the current climate state over North America, relying on simple persistence to extend the "nowcast" into the future for a year or so. Due to the relatively few realizations of the mode in our integration, we shall concentrate for now on the latter description of "prediction."

The keys to nowcasting or specifying the North American climate state associated with the decadal mode are in (i) fixing the phase relation between the mode and its manifestation over North America and (ii) determining, in real time, the current phase of the mode in the ocean–atmosphere system of the Pacific Ocean. These items are demonstrated in turn below.

The phase relation between the North American climate signal and the Pacific decadal mode was obtained from the model output as follows. The modal signature in the oceanic heat content field that is most closely related to the Aleutian low index (and hence climate over North America) was derived by simply lag correlating the SLP index with the gridded heat content field. In this case, the heat content was defined over the range 100–300 m to minimize local coupling effects. The ocean seemed like the logical place to look for the signal given its size and slow evolution. The "best" correlation pattern showed that the induced temperature extremes over the North American continent correspond with conditions wherein the majority of the midlatitude central Pacific has heat content anomalies of one sign. This correlation pattern was then dotted into the original heat content field to make a temporal index of that field that was best related to the future SLP. The heat content index is shown in Fig. 16 together with the SLP index, where the latter has been shifted by four years to best coincide with the heat content index. Thus, knowing the phase of the North Pacific heat content anomaly, one can easily specify the associated SLP and continental temperature pattern expected for the next few years, unless the heat content signal is near a phase transition, in which case no reliable forecast is possible.

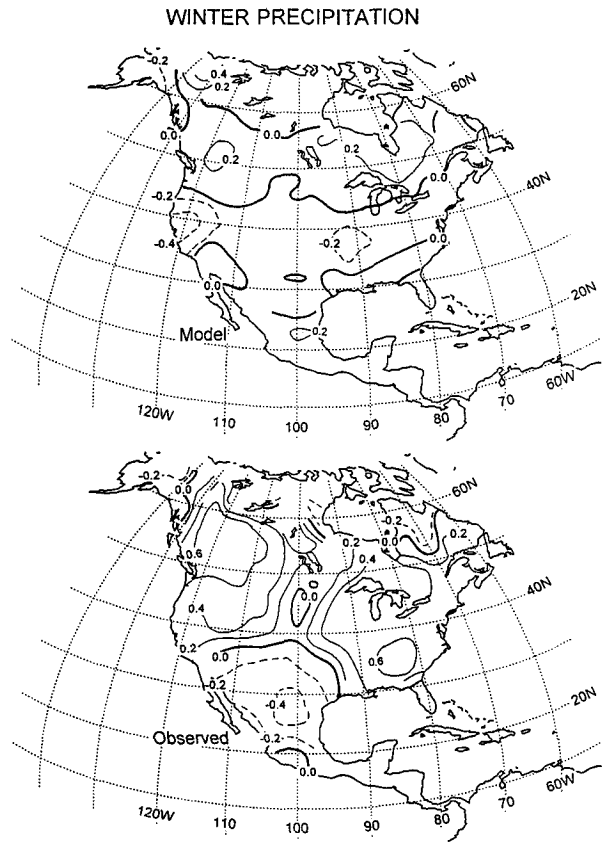

FIG. 14. Correlation of winter sea level pressure anomalies in the Aleutian low region with precipitation anomalies over North America. (a) Upper, as simulated by the ECHO CGCM. (b) Lower, as derived from observations.

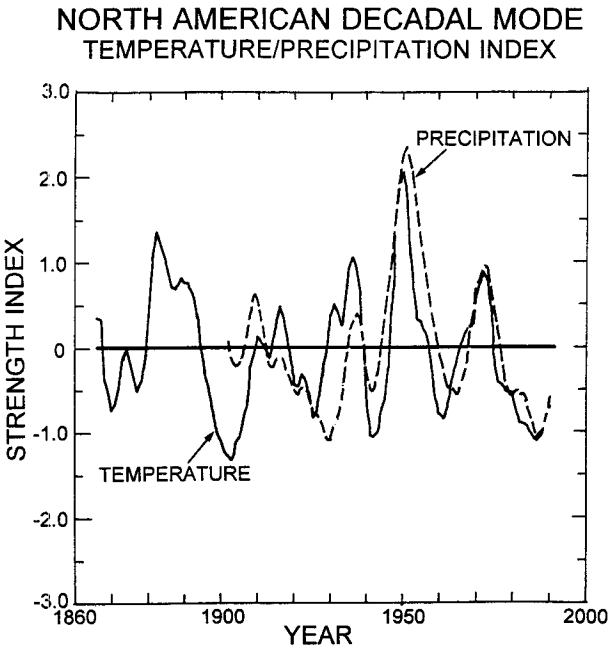

FIG. 15. "Pseudo" principal components for near-surface air temperature (full line) and precipitation anomalies (dashed line) associated with the decadal mode. The two time series were smoothed with a 5-yr running mean filter. See text for further details.

Determining the current state of the decadal mode in the North Pacific is relatively straightforward. The huge spatial extent and long timescale of the mode means that it can be defined with relatively few observations (even in the presence of mesoscale eddy noise in the ocean). There are currently enough expendable bathytermographs (XBTs) being deployed in the North Pacific to define the state of the decadal mode. Fortunately, this situation has existed since at least 1970 (White and Cayan 1996, manuscript submitted to *J. Phys. Oceanogr.*), so one can also investigate the behavior of the mode over the last 20 years. This was accomplished by binning and regriding the XBT data to the OGCM grid and then projecting those data onto the principal heat content correlation pattern obtained from the coupled run, as described above.

The result of projecting the observed heat content anomalies onto the model heat content correlation pattern is shown in Fig. 17. It is clear that since 1970 the heat content of the North Pacific has gone through approximately one complete cycle. We note the rapid phase transition in the mid-1970s, a period that received much attention (e.g., Graham 1994). Our analysis suggests that this "climate shift" was part of the decadal mode. The state of the ocean in 1992, the most recent data used here, is much as it was in the first half of the 1970s. Thus, we might expect a new rapid phase transition, similar to what happened in the mid-1970s.

The forecast methodology described above is only the first crude step in decadal forecasting. A more sophisticated forecasting scheme than that described above could be based on statistical forecasting schemes, such as the POP prediction scheme that would yield a more sophisticated forecast product. Eventually, however, we would like to use coupled GCMs like ECHO to forecast decadal climate variability.

7. Discussion

We have investigated the dynamics and predictability of decadal climate variability over the North Pacific and North America by analyzing observations and the output of a state of the art coupled ocean–atmosphere general circulation model (CGCM). Our results suggest that a considerable part of the decadal variability can be attributed to a cycle with a period of approximately 20 years. The decadal-mode originates from unstable ocean–atmosphere interactions over the North Pacific and must therefore be regarded as an inherently coupled phenomenon. The existence of such a cycle implies the potential for long-range climate forecasting at decadal timescales over North America.

The scenario for the generation of the decadal mode is similar to that developed by Bjerknes (1964) for the Atlantic Ocean. According to this picture, the memory of the coupled system resides in the ocean. The ocean adjusts slowly to past variations in the surface wind stress field, and these slow variations in the wind-driven ocean circulation are crucial in setting the time-

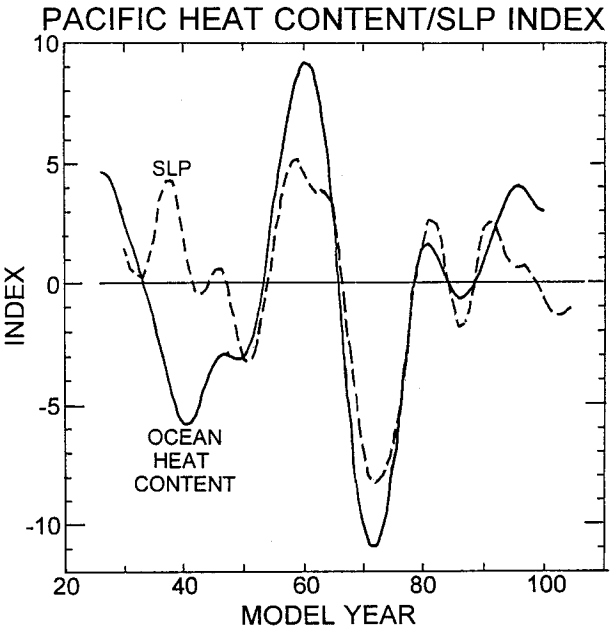

FIG. 16. "Pseudo" principal component of upper-ocean heat content anomalies (full line) over the range 100–300 m and time series of SLP anomalies in the Aleutian low region (dashed line), as derived from the ECHO CGCM. The SLP index was shifted by four years. The two time series were smoothed with a 5-yr running mean filter. See text for further details.

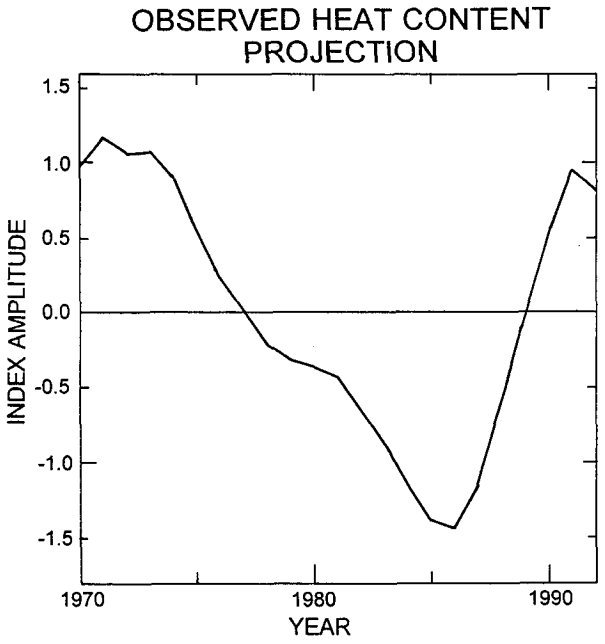

FIG. 17. "Pseudo" principal component obtained by projecting the observed heat content anomalies onto the principal heat content correlation pattern obtained from the coupled run. The time series was smoothed with a 5-yr running mean filter. See text for further details.

scale of the decadal mode. Wave and advective processes are both found to be important in the ocean adjustment. The wave adjustment, however, appears to be the dominant process. The atmosphere responds passively to the changes in the lower boundary conditions. However, since the decadal mode is an inherently coupled phenomenon, the feedback of the atmosphere onto the ocean is a crucial part of the dynamics of the decadal mode.

Our results are in conflict with several previous studies since we found the Tropics played a minor role for the generation of the decadal mode. The studies of Trenberth and Hurrell (1994) and Graham (1994) argue basically that low-frequency changes in tropical Pacific SST introduce the signal into the North Pacific through a changed atmospheric circulation. Jacobs et al. (1994) argues also that decadal variability in the North Pacific is forced by the Tropics, but through the ocean it is forced by the propagation of planetary waves in the aftermath of strong ENSO extremes, such as the 1982–1983 warm event. We did not find much evidence for an active role of the Tropics in the generation of the decadal mode in the North Pacific. Our view of an independent midlatitudinal mode is supported by the findings of Robertson (1996). He investigated a 500-year integration with another CGCM and found a similar mode in the North Pacific to that described here. However, the integration Robertson (1996) analyzed shows virtually no ENSO-type variability in the tropical Pacific so that some of the proposed tropical forcing mechanisms cannot operate in that integration.

Another point of controversy that might originate from our study is the question of whether the atmosphere is sensitive to midlatitudinal SST anomalies. Our results suggest indeed that midlatitudinal SST anomalies force a significant atmospheric response, as implied by the early study of Palmer and Sun (1985). Further, we were able to reproduce the dominant atmospheric response pattern found in the coupled integration and observations by forcing our atmosphere

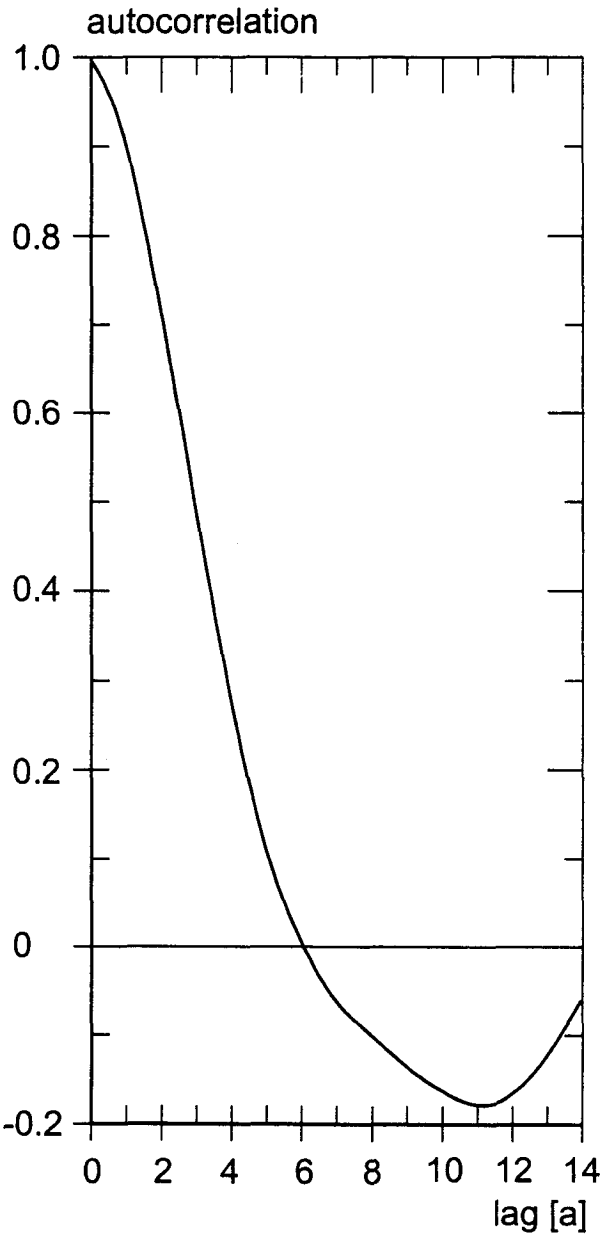

FIG. 18. Autocorrelation function of the near-surface temperature pseudo principal component shown in Fig. 15. The lag is given in years.

model in a stand-alone mode by the characteristic North Pacific SST pattern of the decadal mode. A similar result was obtained by Kumar (1995, personal communication) at the National Meteorological Center. We speculate that changes in the surface baroclinicity and resultant changes in the transient activity are crucial in establishing the time-mean response. If correct, this would imply that atmosphere models need to simulate the eddy activity rather well when they are used in a coupled model in order to study decadal variability. This would require a relatively high resolution for climate integrations, at least of the order of the T-42 resolution we used in our coupled integration.

Finally, we would like to discuss critically the predictability of the decadal mode. Our results suggest that the predictability of the decadal mode is probably less than that on ENSO, for example, if one measures the predictability limits in terms of fractions of the cycle period. This can be inferred from Fig. 18, showing the autocorrelation function of the surface air pseudo principal component (Fig. 15) that was derived by projecting the station data over North America onto the correlation pattern between low-pass filtered North Pacific surface pressure and surface temperature anomalies (Fig. 13). Although the structure of the autocorrelation function shows some weak evidence for a periodicity of approximately 20 years, the correlations at lead times of about 10 years are rather low and of the order of -0.2 only. This suggests that the predictability of the decadal mode is probably considerably less than one-half cycle. In contrast, the autocorrelation functions of typical ENSO indices show significant correlations at lead times of the order of about two years, which corresponds to approximately one-half an ENSO cycle (e.g., Wright 1985). Thus, the decadal "nowcast" or persistence forecast seems to be the most promising approach.

Acknowledgments. We would like to thank Drs. W. White and D. Cayan for many fruitful discussions. Drs. N. Schneider and D. Pierce provided suggestions on an earlier version of the manuscript. We thank Drs. T. Stockdale, J. Wolff, E. Maier-Reimer, and G. Burgers for helping in the development of the coupled model. We thank the Theoretical Applications Division of the Los Alamos National Laboratory for making most of the computer time available for this run, Dr. D. Poling for tending the run and managing the extensive output files, and Dr. C. Keller for facilitating the cooperation on this project. In addition, we thank M. Junge, J. Ritchie, T. Tubbs, and M. Tyree for providing computational assistance. This work was supported in part by the National Science Foundation under Grant NSFATM 9314495, the U.S. Department of Energy's CHAMP program under Grant DE-FG03-91ER61215 (T.P.B.), NOAA via the Lamont/SIO Consortium program, the German Climate Computer Centre (DKRZ), the European Community under Grants EV5V-CT92-0121 and EV5V-CT94-0538, and the Bundesminister für Forschung und Technologie under Grant 07VKV01/1 (M.L.).

REFERENCES

Anderson, D. L. T., and A. E. Gill, 1975: Spinup of a stratified ocean with application to upwelling. *Deep-Sea Res.*, **22,** 583–596.

——, K. Bryan, A. E. Gill, and R. C. Pacanowski, 1979: The transient response of the North Atlantic—Some model studies. *J. Geophys. Res.*, **84,** 4795–4815.

Barnett, T. P., 1985: Variations in near-global sea level pressure. *J. Atmos. Sci.*, **42,** 478–501.

——, 1995: Monte Carlo climate forecasting. *J. Climate,* **8,** 1005–1022.

——, and Coauthors, 1994: Forecasting global ENSO-related climate anomalies. *Tellus,* **46A,** 381–397.

——, M. Latif, N. E. Graham, and M. Flügel, 1995: On the frequency wavenumber structure of the tropical ocean/atmosphere system. *Tellus,* **47A,** 998–1012.

Bjerknes, J., 1964: Atlantic air–sea interaction. *Advances in Geophysics,* Vol. 10, Academic Press, 1–82.

Brankovic, C., T. N. Palmer, and L. Ferranti, 1994: Predictability of seasonal atmospheric variations. *J. Climate,* **7,** 217–237.

Delworth, T., S. Manabe, and R. J. Stouffer, 1993: Interdecadal variations of the thermohaline circulation in a coupled ocean–atmosphere model. *J. Climate,* **6,** 1993–2011.

DKRZ, 1992: The ECHAM-3 atmospheric general circulation model. Tech. Rep. 6, 184 pp. [Available from DKRZ, Bundesstr. 55, D-20146 Hamburg, Germany.]

Gill, A., 1982: *Atmosphere–Ocean Dynamics.* Academic Press, 662 pp.

Graham, N. E., 1994: Decadal-scale climate variability in the 1970s and 1980s: Observations and model results. *Climate Dyn.,* **10,** 135–162.

Hasselmann, K., 1988: PIPs and POPs—The reduction of complex dynamical systems using principal interaction and oscillation patterns. *J. Geophys. Res.,* **93,** 11 015–11 021.

Haston, L., and J. Michaelson, 1994: Long-term central coastal California precipitation variability and relationships to El Niño. *J. Climate,* **7,** 1373–1387.

Horel, H. D., and J. M. Wallace, 1981: Planetary-scale atmospheric phenomena associated with the Southern Oscillation. *Mon. Wea. Rev.,* **109,** 813–829.

Hulme, M., and P. D. Jones, 1993: A historical monthly precipitation dataset for global land areas: Applications for climate monitoring and climate model evaluation. *Analysis Methods of Precipitation on a Global Scale, Report of a GEWEX Workshop,* Koblenz, Germany, World Meteor. Org., A14–A17.

Jacobs, G. A., H. E. Hurlbert, J. C. Kindle, E. J. Metzger, J. L. Mitchell, W. J. Teague, and A. J. Wallcraft, 1994: Decade-scale trans-Pacific propagation and warming effects of an El Niño anomaly. *Nature,* **370,** 360–363.

Jenne, R. L., 1975: Sets for meteorological research. NCAR Tech. Note TN/1A-III, NCAR, Boulder, CO, 194 pp.

Jones, P. D., R. S. Bradley, H. F. Diaz, P. M. Kelly, and T. M. L. Wigley, 1986: Northern Hemisphere surface air temperature variations: 1851–1984. *J. Climate Appl. Meteor.,* **25,** 161–179.

Kushnir, Y., 1994: Interdecadal variations in North Atlantic sea surface temperature and associated atmospheric conditions. *J. Climate,* **7,** 141–157.

Latif, M., and T. P. Barnett, 1994: Causes of decadal climate variability over the North Pacific and North America. *Science,* **266,** 634–637.

——, T. Stockdale, J. O. Wolff, B. Burgers, E. Maier-Reimer, M. M. Junge, K. Arpe, and L. Bengtsson, 1994a: Climatology and variability in the ECHO coupled GCM. *Tellus,* **46A,** 351–366.

——, T. P. Barnett, M. A. Cane, M. Flügel, N. E. Graham, H. von Storch, J.-S. Xu, and S. E. Zebiak, 1994b: A review of ENSO prediction studies. *Climate Dyn.,* **9,** 167–179.

Lau, N.-C., and M. J. Nath, 1994: A modeling study of the relative roles of tropical and extratropical SST anomalies in the variability of the global atmosphere–ocean system. *J. Climate,* **7,** 1184–1207.

Levitus, S., 1982: *Climatological Atlas of the Worlds Ocean.* NOAA Prof. Paper 13, U.S. Govt. Printing Office, Washington, DC, 173 pp. and 17 microfiche.

Mehta, V. M., and T. L. Belworth, 1995: Decadal variability of the tropical Atlantic Ocean in shipboard measurements and in a global ocean–atmosphere model. *J. Climate,* **8,** 172–190.

Miller, A. J., D. C. Cayan, T. P. Barnett, N. E. Graham, and J. M. Oberhuber, 1994: Interdecadal variability of the Pacific Ocean: Model response to observed heat flux and wind stress anomalies. *Climate Dyn.,* **9,** 287–302.

Namias, J., 1959: Recent seasonal interactions between North Pacific waters and the overlying atmospheric circulation. *J. Geophys. Res.,* **64,** 631–646.

——, 1969: Seasonal interactions between the North Pacific and the atmosphere during the 1960s. *Mon. Wea. Rev.,* **97,** 173–192.

Nitta, T., and S. Yamada, 1989: Recent warming of tropical sea surfacetemperature and its relationship to the northern hemisphere circulation. *J. Meteor. Soc. Japan,* **67,** 375–383.

Palmer, T. N., and Z. Sun, 1985: A modelling and observational study of the relationship between sea surface temperature in the northwest Atlantic and the atmospheric general circulation. *Quart. J. Roy. Meteor. Soc.,* **111,** 947–975.

Reynolds, R., 1988: A real-time global sea surface temperature analysis. *J. Climate,* **1,** 75–86.

Robertson, A. W., 1996: Interdecadal variability over the North Pacific in a multi-century climate simulation. *Climate Dyn.,* **12,** 227–241.

Roeckner, E., and Coauthors, 1992: Simulation of the present-day climate with the ECHAM model: Impact of model physics and resolution. Rep. 93, 171 pp. [Available from Max-Planck-Institut für Meteorologie, Bundesstr. 55, D-20146 Hamburg, Germany.]

Schopf, P. S., and M. J. Suarez, 1988: Vacillations in a coupled ocean–atmosphere model. *J. Atmos. Sci.,* **45,** 549–566.

Slutz, R., S. Lubker, J. Hiscoz, S. Woodruff, R. Jenne, D. Joseph, P. Steurer, and D. J. Elms, 1985: Comprehensive Ocean-Atmosphere Data Set: Release I. NOAA Tech. Note NTISPB86-105723, NCAR, Boulder, CO, 268 pp.

Trenberth, K. E., and J. W. Hurrell, 1994: Decadal atmosphere–ocean variations in the Pacific. *Climate Dyn.,* **9,** 303–319.

Venrick, E. L., J. A. McGowan, D. R. Cayan, and T. L. Hayward, 1987: Climate and chlorophyll: Long-term trends in the central North Pacific Ocean. *Science,* **238,** 70–72.

von Storch, H., G. Bürger, R. Schnur, and J.-S. von Storch, 1995: Principal Oscillation Patterns: A review. *J. Climate,* **8,** 377–400.

White, W. B., and T. P. Barnett, 1972: A servomechanism in the ocean–atmosphere system of the midlatitude North Pacific. *J. Phys. Oceanogr.,* **2,** 372–381.

Wright, P. B., 1984: Relationships between indices of the Southern Oscillation. *Mon. Wea. Rev.,* **112,** 1913–1919.